Polaron effects in cylindrical GaAs/$Al_xGa_{1-x}As$ core-shell nanowires*

Hui Sun(孙慧)[1], Bing-Can Liu(刘炳灿)[2], and Qiang Tian(田强)[1,†]

[1] *Department of Physics, Beijing Normal University, Beijing* 100875, *China*
[2] *Department of Fundamental Courses, Academy of Armored Forces Engineering, Beijing* 100072, *China*

(Received 3 February 2017; revised manuscript received 1 June 2017; published online 31 July 2017)

By the fractal dimension method, the polaron properties in cylindrical GaAs/$Al_xGa_{1-x}As$ core-shell nanowire are explored. In this study, the polaron effects in GaAs/$Al_xGa_{1-x}As$ core-shell nanowire at different values of shell width and aluminum concentration are discussed. The polaron binding energy, polaron mass shift and fractal dimension parameter are numerically worked out each as a function of core radius. The calculation results show that the binding energy and mass shift of the polaron first increase and then decrease as the core radius increases, forming their corresponding maximum values for different aluminum concentrations at a given shell width. Polaron problems in the cylindrical GaAs/$Al_xGa_{1-x}As$ core-shell nanowire are solved simply by using the fractal dimension method to avoid complex and lengthy calculations.

Keywords: core-shell nanowire, core radius, polaron effects, fractal dimension

PACS: 73.63.–b, 73.90.+f, 73.63.Nm **DOI:** 10.1088/1674-1056/26/9/097302

1. Introduction

Over the last few years, a lot of experimental research has been done in the low-dimensional semiconductor systems. Polaron effects play important roles in determining various optical and electronic properties observed in these systems. Polaron effects in these systems can be studied simply by using the fractal dimension framework with good accuracy.[1–7] In the past few years, the fractal dimension method has aroused a lot of interest.[1–17] The fractal dimension method proposed by He[1] has been successfully applied to model excitons,[7–11] polarons,[12] and impurities[13–16] in semiconductor materials. Among these materials, core-shell nanowires are extensively regarded as the next frontier in the applications of numerous optoelectronic and electronic equipments.[18–20]

GaAs/$Al_xGa_{1-x}As$ are the important materials mainly used to fabricate these semiconductor nanowires.[21–23] However, few research studies of core-shell nanowires deal with the polaron properties, especially for GaAs/$Al_xGa_{1-x}As$ core-shell nanowires consisting of $Al_xGa_{1-x}As$ core surrounded by GaAs shell, which is of great importance for applications.[18]

The polaron problems in heterostructures are so complicated due to the presence of a variety of phonon modes such as bulk-like phonons, interface phonons, half-space phonons, and slab phonons. Smondyrev *et al.*[24] proposed a simplified polaron model, in which these effects are taken into account. Polaron problems in multilayered heterostructures then can be solved simply by dealing with only one bulk phonon mode and the effective confining potential. On the basis of Smondyrev, Matos-Abiague[4] formulated a more simplified model to solve polaron problems in GaAs/$Al_xGa_{1-x}As$ quantum wells by the fractal dimension method. Then polaron corrections can be calculated by dealing with only one bulk phonon mode and the fractal dimension.

In the present work, we extend the fractal dimension method formulated by Matos-Abiague to the exploration of polaron problems in GaAs shell of GaAs/$Al_xGa_{1-x}As$ core–shell nanowires consisting of $Al_xGa_{1-x}As$ core and GaAs shell. By the fractal dimension method, anisotropic interactions in the real space are assumed as isotropic interactions in an effective fractal dimension environment. The dimension parameter measures the degree of anisotropy in the real physical environment. Accordingly, all relevant anisotropic problems can be solved by introducing a single quantity, i.e., the dimension. Thus we can model the real physical environment in a simple analyzable way by just considering this quantity. During the development of this work, the solution of Schrödinger equation is involved and this is important for solving many problems in physics.[25–28]

The rest of this paper is organized as follows. In Section 2, the fractal dimension method of dealing with the polaron effects in cylindrical GaAs/$Al_xGa_{1-x}As$ core-shell nanowires are explained theoretically. Numeric results and analyses are provided in Section 3. Finally some conclusions are drawn from the present study in Section 4.

2. Model and theory

Now we consider the problem of a bound polaron in a cylindrical GaAs/$Al_xGa_{1-x}As$ core-shell nanowire consisting of $Al_xGa_{1-x}As$ core ($0 \leq r < r_1$) surrounded by GaAs shell ($r_1 \leq r < r_2$). We suppose that no electron can escape from

*Project supported by the National Natural Science Foundation of China (Grant Nos. 10574011 and 10974017).
†Corresponding author. E-mail: qiangtian163@163.com
© 2017 Chinese Physical Society and IOP Publishing Ltd

the structure. The potential of the system is described by

$$V(r)=\begin{cases} V_0, & 0\le r\le r_1,\\ 0, & r_1<r\le r_2,\\ \infty, & r>r_2, \end{cases} \tag{1}$$

where V_0 is the band offset between the conduction bands of core and shell material with the shell width $r_{\rm w}=r_2-r_1$, and r is the radius in the cylindrical coordinate system. The GaAs/Al_xGa_{1-x}As material has a weak electron–LO phonon coupling constant ($\alpha\ll 1$), and we will explore the case of weak coupling. The model of the structure is shown in Fig. 1.

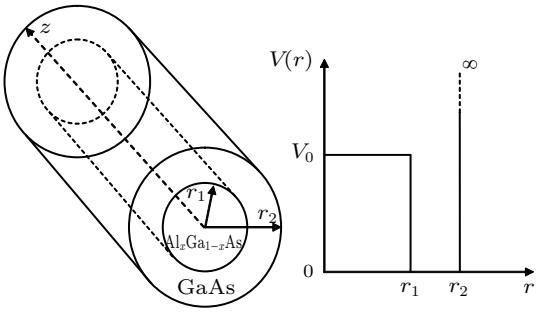


Fig. 1. Model of GaAs/Al_xGa_{1-x}As core-shell nanowire.

Under the effective mass approximation, we write the Schrödinger equation of the system as

$$H_{\rm 3D}\psi_{\rm 3D}(\boldsymbol{r})=E_{\rm 3D}(\boldsymbol{r})\psi_{\rm 3D}(\boldsymbol{r}). \tag{2}$$

Here, $H_{\rm 3D}$ denotes the effective mass Hamiltonian,

$$\mathrm{H_{3D}}=\frac{1}{2}P\frac{1}{m_i}P+V(\boldsymbol{r}), \tag{3}$$

where $P=-\mathrm{i}\hbar\nabla$ is the canonical momentum operator and m_i represents the electron effective mass. Note that

$$m_i=\begin{cases} m_1, & 0\le r\le r_1,\\ m_2, & r_1<r\le r_2. \end{cases} \tag{4}$$

In a cylindrical core-shell nanowire grown along the z direction, the corresponding eigenfunction has the form of

$$\psi_{\rm 3D}(\boldsymbol{r})=C\,\mathrm{e}^{\mathrm{i}k_z z}\psi_{\rm 2D}(r,\varphi), \tag{5}$$

where $C=$ const, φ is the polar angle, and k_z is a quantum number representing the translational symmetry along the z direction. It reduces the complexity of the eigenvalue problem to two coordinates, r and φ,

$$H_{\rm 2D}\psi_{\rm 2D}(r,\varphi)=E\psi_{\rm 2D}(r,\varphi), \tag{6}$$

where

$$H_{\rm 2D}=-\frac{\hbar^2}{2}\left[\frac{1}{r}\frac{\partial}{\partial r}\left(\frac{r}{m_i}\frac{\partial}{\partial r}\right)+\frac{1}{m_i}\frac{1}{r^2}\frac{\partial^2}{\partial\varphi^2}\right]+V(r). \tag{7}$$

We can further reduce the complexity by invoking the axial symmetry,

$$\psi_{\rm 2D}(r,\varphi)=\frac{1}{\sqrt{2\pi}}\mathrm{e}^{\mathrm{i}l\varphi}\psi(r), \tag{8}$$

where l refers to the electron orbital quantum number which denotes the quantized z projection of the angular momentum. The Schrödinger equation for ψ is then

$$\left[\frac{1}{r}\frac{\mathrm{d}}{\mathrm{d}r}\left(\frac{r}{m_i}\frac{\mathrm{d}\psi(r)}{\mathrm{d}r}\right)-\frac{l^2\psi(r)}{m_i r^2}\right]+\left(V(r)+\frac{\hbar^2k_z^2}{2m}\right)\psi(r)=E\psi(r). \tag{9}$$

Since the computation of $k_z\neq 0$ states does not bring any qualitative difference to the obtained results, we only consider the case $k_z=0$. The Schrödinger equation then becomes

$$\left[\frac{1}{m_i}\frac{\mathrm{d}^2\psi(r)}{\mathrm{d}r^2}+\frac{1}{m_i}\frac{1}{r}\frac{\mathrm{d}\psi(r)}{\mathrm{d}r}+\frac{\mathrm{d}}{\mathrm{d}r}\left(\frac{1}{m_i}\right)\frac{\mathrm{d}\psi(r)}{\mathrm{d}r}-\frac{l^2\psi(r)}{m_i r^2}\right]+V(r)\psi(r)=E\psi(r). \tag{10}$$

By means of the fractal dimension method, the polaron in actual low-dimensional structure is transformed into free polaron in a fractal dimension system. On the basis of second-order perturbation theory, polaron corrections in fractal dimension can be obtained. The polaron energy shift can be calculated from[2–5]

$$\Delta E=\alpha\hbar\omega_{\rm LO}G_1(D), \tag{11}$$

and we have the effective mass of the polaron as[2–5]

$$m^*=\frac{m}{1-\alpha G_2(D)}. \tag{12}$$

In Eqs. (11) and (12), $\omega_{\rm LO}$ refers to LO-phonon limiting frequency approximation without dispersive effects, D indicates the fractal dimension, α is the Fröhlich constant, m is the effective mass of electron, functions $G_1(D)$ and $G_2(D)$ depending on D are obtained from

$$G_1(D)=\frac{\sqrt{\pi}}{2}\frac{\Gamma\left[(D-1)/2\right]}{\Gamma\left[D/2\right]}, \tag{13a}$$

and

$$G_2(D)=\frac{\sqrt{\pi}}{4}\frac{\Gamma\left[(D-1)/2\right]}{D\Gamma\left[D/2\right]}. \tag{13b}$$

In Eqs. (13) and (14), $\Gamma(x)$ refers to the Gamma function. The fractal dimensionality of our system is determined by[2–5]

$$D=3-2\exp\left(\frac{L_{\rm w}^*}{2R_{\rm p}}\right), \tag{14}$$

where $L_{\rm w}^*$ is the effective length of the quantum confinement, $R_{\rm p}=\sqrt{\hbar/2m\omega_{\rm LO}}$ is the radius of the polaron. In terms of our system, the effective length has the form

$$L_{\rm w}^*=2\left(r_{\rm w}+\frac{1}{k_1}\right), \tag{15}$$

where k_1 refers to the electron wave vector in core and it can be obtained from the relationship

$$k_1 = \frac{\sqrt{2m_1(V_0 - E)}}{\hbar}. \tag{16}$$

The ground state eigenenergy E of the electron is then obtained by solving the Schrödinger equation (10).

In a cylindrical GaAs/$Al_xGa_{1-x}As$ core-shell nanowire, the material parameters characterizing the polaron properties in the core are different from those in the shell. Taking into account this problem, we introduce the average parameter method over all the effective fractal dimension regions. The average parameter values of the material which characterize the fractal dimension electron–phonon interaction have the forms[4]

$$m^{-1} = \sum_{i=1,2} \frac{P_i}{m_i}, \tag{17}$$

$$\omega_{\mathrm{LO}} = \sum_{i=1,2} \omega_i P_i, \tag{18}$$

and

$$\alpha = \left[\sum_{i=1,2} \left(P_i \frac{\omega_i}{\omega_{\mathrm{LO}}} \sqrt{\alpha_i \sqrt{\frac{m\omega_{\mathrm{LO}}}{m_i \omega_i}}} \right) \right]^2, \tag{19}$$

$$R_{\mathrm{p}} = \left[\sum_{i=1,2} \left(P_i \frac{\omega_i}{\omega_{\mathrm{LO}}} \sqrt{\frac{\alpha_i R_{\mathrm{p}i}}{\alpha}} \right) \right]^2, \tag{20a}$$

$$R_{\mathrm{p}i} = \sqrt{\frac{\hbar}{2m_i\omega_i}}. \tag{20b}$$

In Eqs. (17)–(20), ω_i represent the phonon frequencies, α_i are the Fröhlich constants in different regions, and

$$P_1 = \int_0^{r_1} |\psi(r)|^2 \mathrm{d}r, \tag{21a}$$

$$P_2 = 1 - P_1, \tag{21b}$$

represent the appearance chances of the electron in core ($Al_xGa_{1-x}As$) and shell (GaAs) regions. The polaron binding energy and mass shift in cylindrical GaAs/$Al_xGa_{1-x}As$ core-shell nanowire then can be calculated in a quick and simple manner according to Eqs. (11), (12), and (14). Then the shell-width-dependent polaron properties can be obtained on the basis of the average material parameters given by Eqs. (17)–(21).

3. Numeric results and analyses

As a function of the core radius in the GaAs/$Al_xGa_{1-x}As$ core-shell nanowire for different Al content at a given shell width $r_{\mathrm{w}} = 40$ Å, the polaron binding energies are worked out and shown in Fig. 2. The data show that the corresponding numeric values first increase at different Al content as core radius r_1 increases. Then the binding energies decrease monotonically as core radius continues to increase. For large core radius the polaron binding energy stays constant over the whole range. The maximum values appear at the $Al_xGa_{1-x}As$ core radius $r_1 = 23$ Å for $x = 0.35$, $r_1 = 28$ Å for $x = 0.3$, and $r_1 = 40$ Å for $x = 0.25$, respectively. The same behavior of the core-radius-dependent polaron mass shift $m = (m^* - m)/(m_2^* - m_2)$ is observed in Fig. 3. It is worth noting that different Al content obviously affects the polaron binding energy and mass shift over all the core radius range. Their values decrease with decreasing aluminum content.

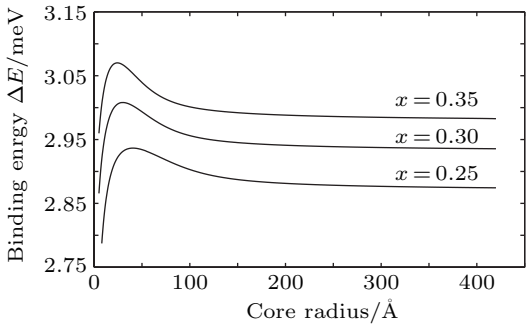


Fig. 2. Variations of fractal dimension polaron binding energy with core radius in GaAs/$Al_xGa_{1-x}As$ core-shell nanowire at the shell width $r_{\mathrm{w}} = 40$ Å.

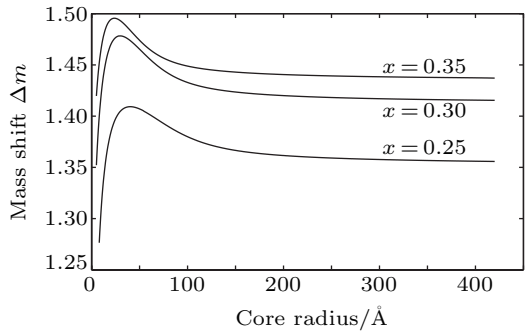


Fig. 3. Variations of fractal dimension polaron mass shift with core radius in GaAs/$Al_xGa_{1-x}As$ core-shell nanowire at the shell width $r_{\mathrm{w}} = 40$ Å.

Figures 2 and 3 show that the polaron binding energy and mass shift first increase with increasing core radius, reaching their maximum values and then decrease. It is noted that this behavior is predicted by the research of a polaron confined in the finite-potential quantum wire.[9]

As a function of the core radius, the values of fractal dimension parameter D relating to Figs. 2 and 3 are shown in Fig. 4. In Fig. 4, we can see that the fractal dimension is not sensitive to the change of core radius over the whole range. It is easy for us to explain this phenomenon. The core radius, to some extent, does not exert much influence on the fractional dimension because the main polaron wave function is constrained inside the shell. Figure 4 shows that the fractal dimension tends to be a constant for very large core radius. As the core radius decreases, the fractal dimension first increases slowly, reaching peaks at the core radius $r_1 = 40$ Å for

$x = 0.35$, $r_1 = 45$ Å for $x = 0.3$, and $r_1 = 72$ Å for $x = 0.25$, respectively. Then the fractal dimension decreases slowly as core radius continues to decrease.

In order to prove that the numeric results are reasonable, we consider the limit case. When the core radius is very large, we take $x = 0.3$ for example, and the cylindrical GaAs/Al_xGa_{1-x}As core-shell nanowire system is the same as a GaAs thin film quantum well with $Al_{0.3}Ga_{0.7}As$ finite barriers for a polaron. In Fig. 4, we can see that the fractal dimension tends to be 2.627 ($D \approx 2.627$) when the core radius is very large. The polaron binding energy and polaron mass shift corresponding to $D \approx 2.627$ can be found in Figs. 2 and 3. Their numerical results are $E \approx 2.94$ meV and $m \approx 1.42$, respectively, which are consistent with the results given by Matos-Abiague[4] for the same fractal dimension parameter.

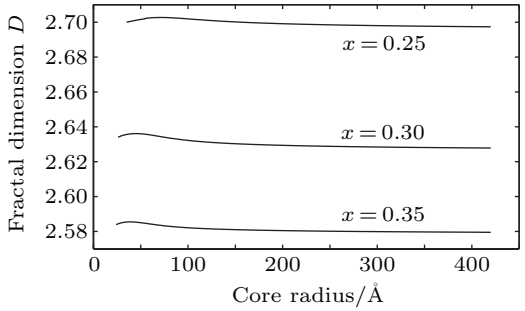


Fig. 4. Variations of corresponding fractal dimension with core radius in GaAs/Al_xGa_{1-x}As core-shell nanowire at the shell width $r_w = 40$ Å.

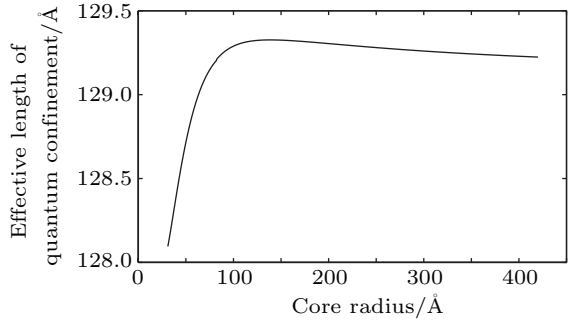


Fig. 5. Effective length of the quantum confinement versus core radius in GaAs/Al_xGa_{1-x}As core-shell nanowire for $x = 0.3$ at the shell width $r_w = 40$ Å.

Furthermore, in order to explain the change regularity of the fractal dimension clearly, we relate the effective length of the quantum confinement to polaron diameter as displayed in Figs. 5 and 6. In Fig. 5, we can see that the effective length of the quantum confinement first increases when core radius decreases for large core radius. This is because the decrease of core radius causes the decrease of the whole core-shell nanowire radius r_2, and then leads to enhanced confinement effect of the polaron. Thus the polaron wave function will spread into the core, causing the effective length of the quantum confinement to increase. Moreover, increasing effective length of the quantum confinement will lead to increasing fractal dimension parameter. When the core radius is reduced to a small enough value, the effective length of the quantum confinement decreases for polaron to tunnel the core.

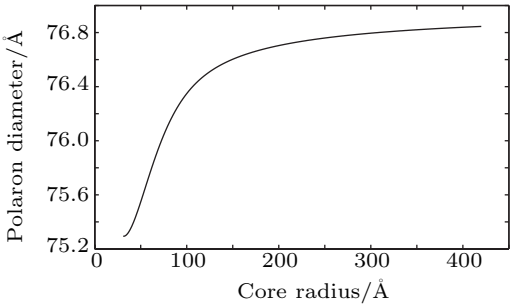


Fig. 6. Polaron diameter versus core radius in GaAs/Al_xGa_{1-x}As core-shell nanowire for $x = 0.3$ at the shell width $r_w = 40$ Å.

In Figs. 5 and 6, we take the Al content $x = 0.3$ for example. As indicated in Eq. (15), the fractal dimension is determined by the effective length of quantum confinement and polaron diameter. A comparison between Figs. 5 and 6 shows that for large core radius $r_1 > 138$ Å the effective length of quantum confinement increases with core radius decreasing. On the other hand, the polaron diameter decreases as core radius decreases over the whole range, for the polaron becomes increasingly confined and compressed. Thus the effective fractal dimension increases as core radius decreases in the region $r_1 > 138$ Å. When $r_1 \leq 138$ Å, both the effective length of quantum confinement and polaron diameter decrease as core radius decreases. However, in the region 45 Å$\leq r_1 \leq 138$ Å, the polaron diameter decreases more intensely than the effective length of quantum confinement. Consequently, the fractal dimension continues to increase as core radius decreases in this region and reaches a peak value at the core radius $r_1 = 45$ Å. In the region $r_1 < 45$ Å, the scenario is just opposite, the effective length of quantum confinement decreases more intensely and the fractal dimension begins to decrease finally.

In Figs. 2–4, we can see that the peaks of polaron binding energy, mass shift and fractal dimension drop with increasing the Al content in the core. The values of polaron binding energy and mass shift rise as Al content increases for narrow shell width, while the fractal dimension behaves in the opposite way.

The variation relationships between core radius and the polaron binding energy in the GaAs shell at different values of $Al_{0.3}Ga_{0.7}As$ and shell widths $r_w = 30$, 35, 40 Å, are shown in Fig. 7. Corresponding function relationships of polaron mass shift are shown in Fig. 8. In the case of different shell widths, the curves of polaron binding energy and mass shift also first increase for different Al content as core radius r_1 increases. Then they decrease as the core radius continues to increase.

Their maximum values appear at the $Al_xGa_{1-x}As$ core radii of 72, 40, and 30 Å, respectively. From Figs. 7 and 8, we notice that the values of polaron binding energy and mass shift drop as shell width decreases.

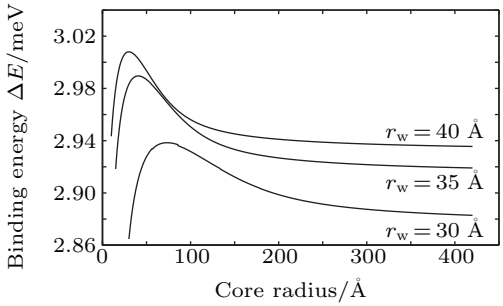


Fig. 7. Variations of fractal dimension polaron binding energy with core radius in $GaAs/Al_{0.3}Ga_{0.7}As$ core-shell nanowire at different values of shell width $r_w = 30$, 35, 40 Å, respectively.

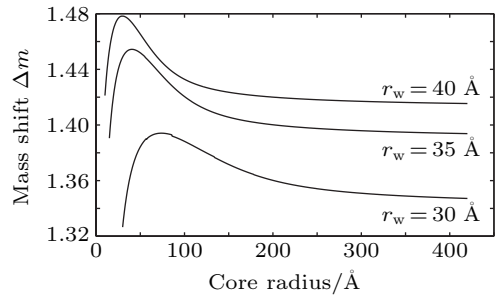


Fig. 8. Variations of fractal dimension polaron mass shift with the core radius in $GaAs/Al_{0.3}Ga_{0.7}As$ core-shell nanowire at different values of shell width $r_w = 30$, 35, 40 Å, respectively.

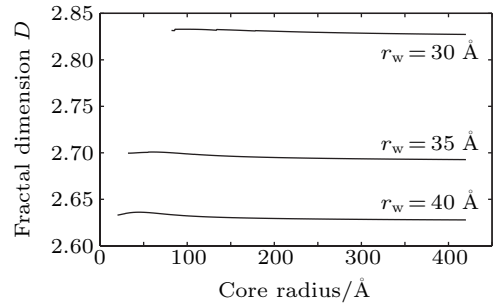


Fig. 9. Variations of corresponding fractal dimension with core radius in $GaAs/Al_{0.3}Ga_{0.7}As$ core-shell nanowire at different values of shell width $r_w = 30$, 35, 40 Å, respectively.

The plots of fractal dimension parameter D versus core radius for different shell width values, corresponding to Figs. 7 and 8 are displayed in Fig. 9. For different values of the shell width, we can see that the fractal dimension tends to be a constant for very large core radius. As the core radius decreases, the values of fractal dimension first increase slowly, reaching their peaks at core radii $r_1 = 90$ Å for $r_w = 30$ Å, $r_1 = 60$ Å for $r_w = 35$ Å, and $r_1 = 45$ Å for $r_w = 40$ Å, respectively. Then the fractal dimension decreases slowly and continues to decrease as core radius increases. Remarkably, the data in Fig. 9 show that the core radius, in a certain range, does not exert much influence on fractional dimension. However, the shell width has a more significant influence on fractional dimension for the three non-overlapping discrete curves, because the main polaron wave function is constrained inside the shell and the change of shell width will influence the effective length of the quantum confinement directly.

4. Conclusions

We present for the first time the polaron binding energy and mass shift in $GaAs/Al_xGa_{1-x}As$ core–shell nanowires. We use the fractal dimension method, with which the actual $GaAs/Al_xGa_{1-x}As$ core–shell nanowire is taken as an effective fractal dimension system. In this system, the polaron is assumed to behave in an unconfined manner. The fractal dimension measures the extent of the confinement in the real environment. In this case, polaron effects in $GaAs/Al_xGa_{1-x}As$ core–shell nanowires at different values of shell width and aluminum content are studied. The fractal dimension method allows the polaron properties such as polaron binding energy and mass shift to be measured in a simple analyzable way, avoiding complex calculations caused by traditional methods. In this article, core-radius-affected polaron binding energy and mass shift are obtained for $GaAs/Al_xGa_{1-x}As$ core–shell nanowire. It shows that both the polaron binding energy and mass shift initially rise by raising the core radius, reaching a maximum, and then decrease as the core radius in $GaAs/Al_xGa_{1-x}As$ core-shell nanowires continues to increase. Our calculations have some reference values for the change regulations of optical and electronic properties when the core radius or shell width changes, which are important properties of the $GaAs/Al_xGa_{1-x}As$ core-shell nanowires.[20,29,30]

References

[1] He X F 1991 *Phys. Rev. B* **43** 2063
[2] Matos-Abiague A 2002 *J. Phys. Condens. Matter* **14** 4543
[3] Matos-Abiague A 2002 *Semicond. Sci. Technol.* **17** 150
[4] Matos-Abiague A 2002 *Phys. Rev. B* **65** 165321
[5] Wu Z H, Li H, Yan L X, Liu B C and Tian Q 2013 *Physica B* **410** 28
[6] Wu Z H, Li H, Yan L X, Liu B C and Tian Q 2013 *Superlattices Microstruct.* **55** 16
[7] Li H, Liu B C, Shi B X, Dong S Y and Tian Q 2015 *Front. Phys.* **10** 107302
[8] Wu Z H, Chen L and Tian Q 2015 *Int. J. Mod Phys B* **29** 1550213
[9] Vartanian A L, Asatryan A L and Vardanyan L A 2013 *Physica E* **47** 134
[10] Christol P, Lefebvre P and Mathieu H 1993 *J. Appl. Phys.* **5626** 74
[11] Lefebvre P, Christol P and Mathieu H 1992 *Phys. Rev. B* **46** 13603
[12] Thilagam A and Matos-Abiague A 2004 *J. Phys.: Condens. Matter* **16** 3981
[13] Gómez E R, Oliveira L E and de Dios-Leyva M 1999 *J. Appl. Phys.* **85** 4045
[14] Mikhailov I D, Betancur F J, Escorcia R A and Sierra-Ortega J 2003 *Phys. Rev. B* **67** 115317
[15] Kundrotas J, Cerškus A, Ašmontas S, Valusis G, Sherlikerl B and Harrison M P 2005 *Phys. Rev. B* **72** 235322
[16] Kundrotas J, Cerškus A, Ašmontas S, Valušis G, Halsall M P, Johannessen E and Harrison P 2007 *Semicond. Sci. Technol.* **22** 1070
[17] Gao J and Zhang M C 2016 *Chin. Phys. Lett.* **33** 010303

[18] Mayer B, Rudolph D, Schnell J, Morkötter S, Winnerl J, Treu J, Müller K, Bracher G, Abstreiter G, Koblmüller G and Finley J J 2013 *Nat. Commun.* **4** 2931
[19] Lubk A, Wolf D, Prete P, Lovergine N, Niermann T, Sturm S and Lichte H 2014 *Phys. Rev. B* **90** 125404
[20] Morkötter S, Jeon N, Rudolph D, Loitsch B, Spirkoska D, Hoffmann E, Döblinger M, Matich S, Finley J J, Lauhon L J, Abstreiter G and Koblmüller G 2015 *Nano Lett.* **15** 3295
[21] Jiang N, Parkinson P, Gao Q, Breuer S, Tan H H, Wong-Leung J and Jagadish C 2012 *Appl. Phys. Lett.* **101** 023111
[22] Rudolph D, Funk S, Döblinger M, Morkötter S, Hertenberger S, Schweickert L, Becker J, Matich S, Bichler M, Spirkoska D, Zardo I, Finley J J, Abstreiter G and Koblmüller G 2013 *Nano Lett.* **13** 1522
[23] Aciksoz E, Bayrak O and Soylu A 2016 *Chin. Phys. B* **25** 100302
[24] Smondyrev M A, Gerlach B and Dzero M O 2000 *Phys. Rev. B* **62** 16692
[25] Cheng R J and Cheng Y M 2016 *Chin. Phys. B* **25** 020203
[26] Song X D, Dong S H and Zhang Y 2016 *Chin. Phys. B* **25** 050302
[27] Khalid S A 2014 *Chin. Phys. Lett.* **31** 120301
[28] Diwaker and Chakraborty A 2015 *Chin. Phys. Lett.* **32** 070301
[29] Hocevar M, Giang L T T, Songmuang R, Hertog M D, Besombes L, Bleuse J, Niquet Y and Pelekanos N T 2013 *Appl. Phys. Lett.* **102** 191103
[30] Songmuang R, Giang L T T, Bleuse J, Hertog M D, Niquet Y M, Dang L S and Mariette H 2016 *Nano Lett.* **16** 3426